Tetrahedron 64 (2008) 5384–5391

Contents lists available at ScienceDirect

Tetrahedron

journal homepage: www.elsevier.com/locate/tet

# Synthesis of new tripodal receptors—a 'PET' based 'off–on' recognition of $Ag^+$

Vimal K. Bhardwaj, Ajay Pal Singh Pannu, Narinder Singh, Maninder Singh Hundal, Geeta Hundal *

*Department of Chemistry, Guru Nanak Dev University, Amritsar 143005, Punjab, India*

ARTICLE INFO

*Article history:*
Received 2 October 2007
Received in revised form 7 February 2008
Accepted 6 March 2008
Available online 18 March 2008

ABSTRACT

A new set of tripodal receptors based upon an aromatic platform have been synthesized in high yields. The compounds have been characterized by spectroscopic techniques and by single crystal X-ray crystallography. These receptors are found to have good extraction ability and high transport rate for Ag(I). The receptor with imine linkages exhibits weak fluorescence emission bands at $\lambda_{max}$=413 and 540 nm, upon excitation at $\lambda_{max}$=365 nm. The fluorescence spectrum of the receptor shows enhancement in the intensity of the signal at 413 nm on binding with the $Ag^+$ cation. No such significant changes are observed with other metal ions. An absorption at ~365 nm is typical of an intraligand ($\pi$–$\pi^*$) transition involving the imine chromophore, which produces a weak emission band at 413 nm due to quenching caused by PET from a neighboring –OH group. Participation of OH group in coordination to the metal ion reduces PET and an enhancement of fluorescence intensity is observed, signaling recognition of the metal ion.



## 1. Introduction

Currently the synthesis of fluorescent sensors for heavy transition metal ions (HTM) is gaining impetus because of their biological and environmental importance.[1] There are numerous reported examples of fluoroionophores, which show excellent selectivity for heavy metals,[2] especially $Hg^{2+}$ and $Cu^{2+}$ ions. However, the quenching nature of HTM via spin–orbit coupling or via energy/electron transfer poses[3] a disadvantage in high signal output. The known receptors for HTM are now being based upon chelation induced quenching (CHEQ) or enhancement of fluorescence (CHEF) phenomenon.[4] Quenching of fluorescence by metal ion during complexation is a common phenomenon whereas enhancement is rare and of much interest as it opens up the opportunity for photochemical applications of these complexes.[5] For sensing of a single analyte, the use of the receptor–spacer–reporter paradigm is one of the good approaches.[6] In this approach a receptor is covalently bonded to a reporter, which may be a chromophore/fluorophore.[7] If the spacer is not long, the receptor and reporter may overlap in identity[8] but there must exist some mechanism by which the reporter can transduce the binding of the analyte to the receptor. This approach has been used to obtain many chromogenic/fluorogenic receptors for different metal ions.[2] A number of reports have appeared lately on the prospective use of fluorescence characteristics on transition metal complexation of Schiff base ligands having no other fluorophore (reporter) in the chemosensor except for the imine group.[9] These examples mainly include small dipodal ligands based on salicylidimine unit. Therefore in our ongoing work on tripodal receptors containing Schiff bases[10] we have exploited the fluorescence capability of a newly synthesized tripodal Schiff base where the imine group may behave as a receptor and/or a reporter. Both, the amine **2** and the Schiff base **3**, have showed good recognition for $Ag^+$ ion with the latter also showing selectivity for the $Ag^+$ ion. To the best of our knowledge there are only a few fluorogenic sensors[11] known for Ag(I) ion, therefore this piece of work further gains importance.

## 2. Synthesis and spectroscopic characterization

Compound **1** was prepared by the reported method.[12] Receptor **2** was synthesized by the reaction of tripodal bromide **1** with 2-aminothiophenol under phase transfer catalytic and dry conditions. A condensation reaction of tripodal amine **2** with salicylaldehyde, in the presence of catalytic amount of zinc perchlorate[10b] gave receptor **3** in good yields (Scheme 1). The compounds were characterized by elemental analyses and spectroscopic techniques. Receptors **2** and **3** were also characterized by single crystal X-ray diffraction methods. A peak at $\delta$ 4.36 in the $^1$H NMR of **2** clearly indicates the $-NH_2$ protons. Since there is one peak each for $-CH_3$, $-CH_2$, $-CH_2S$ protons and for each of the aromatic protons, this indicates that the tripodal **2** is present in a cis, cis, cis conformation [10c,13] in the solution phase. In the IR spectrum bands at around 3388, 3469 $cm^{-1}$ characterized the presence of the amine group in the molecule. Similarly for receptor **3**, a sharp peak at 1613 $cm^{-1}$ and a broad peak at 3419 $cm^{-1}$ in the IR spectrum indicates the presence of an imine group and a H-bonded –OH group present in the compound **3**. The same were established by the presence of

* Corresponding author. Tel.: +91 183 250 2113; fax: +91 183 225 8820.
*E-mail address:* geetahundal@yahoo.com (G. Hundal).

0040-4020/$ – see front matter © 2008 Elsevier Ltd. All rights reserved.
doi:10.1016/j.tet.2008.03.013

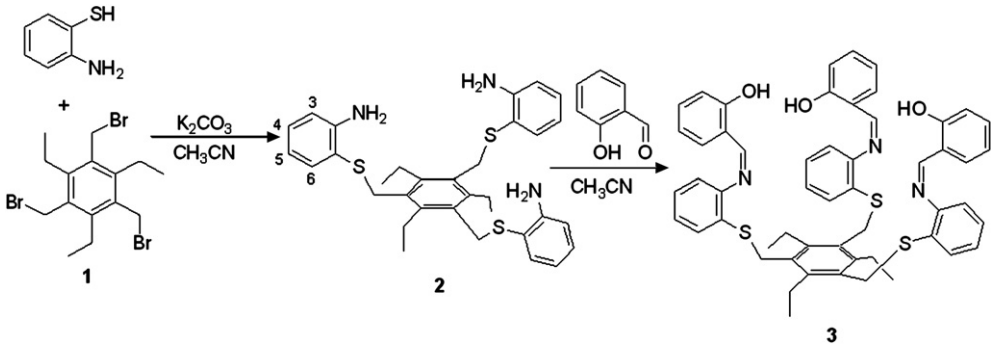


**Scheme 1.**

signals at $\delta$ 8.55 and 13.14 in the $^{1}$H NMR spectrum and at $\delta$ 162.42 and 172.63 in $^{13}$C NMR spectra, respectively. The chemical shift of the hydroxyl protons is typical for the resonance-assisted hydrogen-bonded (RAHB) proton of O–H···N=C.[14] The CHN data are also in accordance with the molecular formulae.

## 3. X-ray crystal structure studies

Table 1 shows the cell parameters and refinement parameters for **2** and **3**. The solid state structure of **2** is shown in Figure 1. The molecule is in the cis, cis, cis conformation.[10c,13] The four aromatic rings are planar. The ring B (C8–C13), ring C (C17–C22), and the ring D (C26–C31) have dihedral angles of 16.3(1), 71.3(1), 33.6°(1) with ring A (C1–C6), respectively. Torsion angles about S1–C7, S2–C16, and S3–C25 are 176.5(3), 177.9(2), and −63.4°(3), respectively. Thus the aromatic rings B and C are in an extended conformation with respect to ring A but ring D has taken a twist toward the central ring A (Fig. 2). This change in conformation may be due to the C–H···$\pi$ interaction between C27–H27···centroid of ring A at 3.88 Å. Any threefold symmetry found in the solution phase has been destroyed because of the different orientations of the three arms of the tripods.

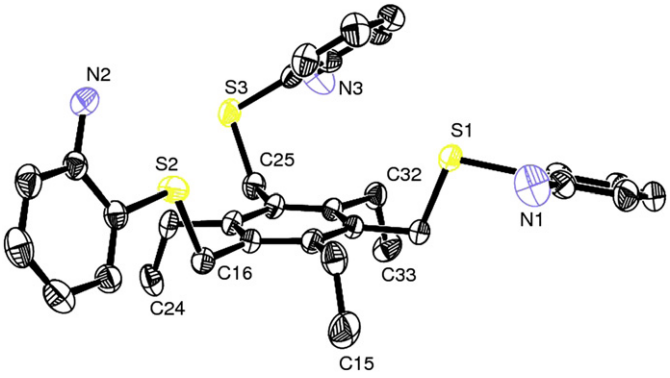


**Figure 1.** Showing the ORTEP diagram of (**2**) and the labeling scheme used.

**Table 1**
Crystal data and structure refinement for **2** and **3**

| Identification code | **2** | **3** |
|---|---|---|
| Empirical formula | $C_{33}H_{39}N_3S_3$ | $C_{54}H_{51}N_3O_3S_3$ |
| Formula weight | 573.85 | 886.16 |
| Temperature (K) | 295(2) | 295(2) |
| Wavelength (Å) | 0.71069 | 0.71069 |
| Crystal system | Orthorhombic | Triclinic |
| Space group | *Pna*2$_1$ | *P*-1 |
| Unit cell dimensions | *a*=16.063(5) Å | *a*=11.98(4) Å |
| | *b*=10.920(5) Å | *b*=12.595(18) Å |
| | *c*=18.327(5) Å | *c*=15.91(2) Å |
| | $\alpha$=90.0° | $\alpha$=82.02(10)° |
| | $\beta$=90.0° | $\beta$=87.26(18)° |
| | $\gamma$=90.0° | $\gamma$=81.44(16)° |
| Volume (Å$^3$) | 3215(2) | 2350(8) |
| *Z* | 4 | 2 |
| Density (calculated) (Mg/m$^3$) | 1.186 | 1.252 |
| Absorption coefficient (mm$^{-1}$) | 0.256 | 0.205 |
| *F*(000) | 1224 | 936 |
| Crystal size (mm$^3$) | 0.22×0.20×0.20 | 0.21×0.18×0.19 |
| Theta range for data collection (°) | 2.17–26.00 | 1.29–25.50° |
| Index ranges | $-1\le h\le 19$ | $0\le h\le 12$ |
| | $-1\le k\le 13$ | $-14\le k\le 15$ |
| | $-22\le l\le 25$ | $-19\le l\le 19$ |
| Reflections collected | 7520 | 8947 |
| Independent reflections | 6318 [*R*(int)=0.0225] | 8500 [*R*(int)=0.0620] |
| Completeness to theta=26.00° (%) | 100.0 | 97.0 |
| Absorption correction | None | None |
| Refinement method | Full-matrix least-squares on $F^2$ | |
| Data/restraints/parameters | 6318/1/352 | 8500/0/568 |
| Goodness-of-fit on $F^2$ | 0.933 | 0.807 |
| Final *R* indices [$I>2\sigma(I)$] | *R*1=0.0543 | *R*1=0.0861 |
| | *wR*2=0.1380 | *wR*2=0.1945 |
| *R* indices (all data) | *R*1=0.0816 | *R*1=0.2330 |
| | *wR*2=0.1501 | *wR*2=0.2993 |
| Absolute structure parameter | 0.00(8) | — |
| Largest diff. peak and hole (e Å$^{-3}$) | 0.762 and −0.234 | 0.511 and −0.568 |
| CCDC No. | 662439 | 662440 |

Inter and intra-molecular H-bonding interactions were found in the unit cell (Table 1 in Supplementary data). The amine nitrogens are intra-molecularly H-bonded to sulfur atoms in their respective arms. Inter-molecular N1···N2 H-bonding forms helical, polymeric chains running parallel to the *a* axis. These parallel helical chains are linked to each other via N1···N3 H-bonding extending the network in the *ac* plane (Fig. 3). Thus the crystal structure comprises of cross-linked helices down the *b* axis.

The X-ray crystal structure of **3** is shown in Figure 4. All seven aromatic rings are almost planar with maximum deviation of

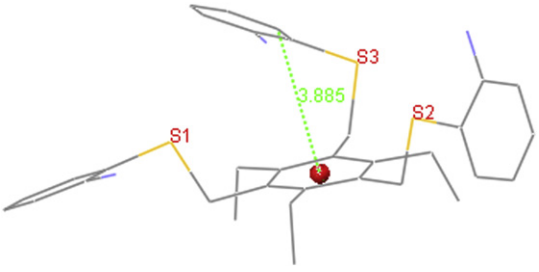


**Figure 2.** Showing one of the arms of the tripod being turned inside to come above the ring A.

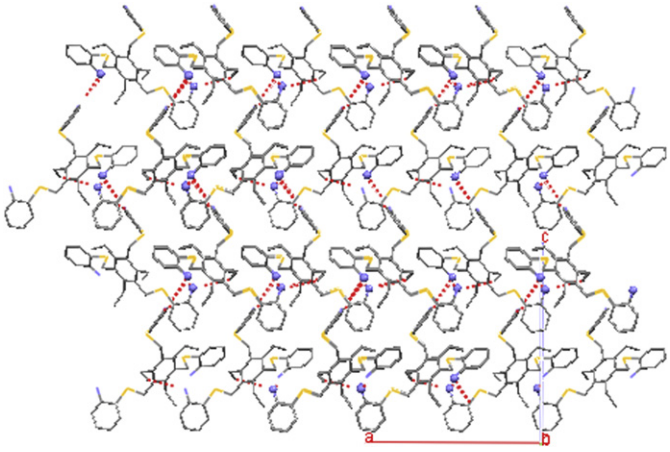


**Figure 3.** Showing cross-linked helices in the *ac* plane.

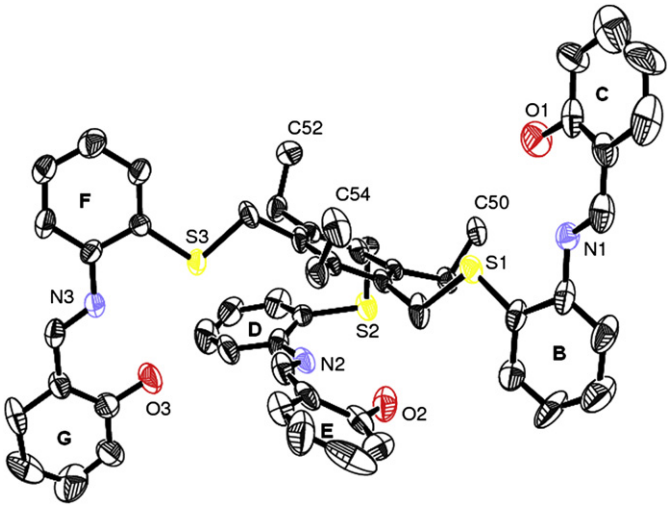


**Figure 4.** Showing ORTEP of compound **3** and its partial labeling scheme. Hydrogens and labels of carbon atoms have been removed for clarity.

0.05 Å for the central ring (ring A). One arm of the tripod is highly unsymmetrical with respect to the other two, thus removing any threefold symmetry expected of the compound as found in the solution phase. The rings B (C8–C13), D (C22–C27), and F (C36–C41) have dihedral angles of 91, 144, and 94° with ring A, respectively. Similarly ring C (C15–C20) and ring G (C43–C48) are perpendicular (dihedral angles 101 and 93°, respectively) but ring E (C29–C34) is parallel (dihedral angle 174°) with respect to ring A. The torsion angles S1–C7 and S3–C35 are anti, being −169 and −174°, respectively, but S2–C21 is *gauche* 78°. These values show that the tripod is not in its fully extended form but one of its arms is folded to make a loop with ring E parallel to ring A. This loop is further stabilized by many intramolecular interactions such as C–H···π interactions between methylene C7 and ring E (3.709 Å) and imine C28 and ring A (3.459 Å), edge to edge π···π interactions between ring A and D, H-bonding between methylene C7 and O2 and C49 and S2, imine C28 and O3, phenylene C26 and O3, methylene C51 and C53, with S3 and methyl C54 and S1 (Table 2 in Supplementary data).

There are other intra and inter-molecular H-bonding interactions found in the unit cell. The hydroxyl oxygens O1 and O3 are acting as double H-bond donors to imine nitrogens N1 and N3 and thioether sulfurs S1 and S3, respectively, in the two extended arms. However, in the folded arm of the tripod, O2 forms intramolecular H-bonding with imine nitrogen N2, but not to S2. A very similar conformation has earlier been reported by us for a similar mesitylene based tripodal ligand.[10a] The crystal structure of the compound shows the formation of C–H···π based, centrosymmetric dimeric molecules (C17–H17···centroid of ring G$^{ii}$ 3.45(3) Å), which are further joined to each other due to π···π bonding (C42–H42··· centroid of ring F$^{v}$ 3.80(4) Å) forming polymeric chains running diagonally in the *ac* plane (Fig. 5).

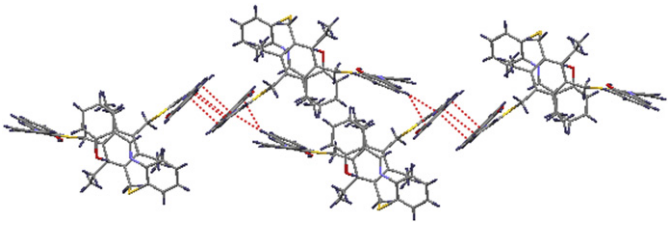

**Figure 5.** Showing formation of polymeric chains due to C–H···π and π···π bonding.

## 4. Fluorescence studies

Receptor **3** shows a broad absorption band (Fig. 6) at $\lambda_{max}$=355 nm in the absorption spectrum, which is due to an intraligand π···π* transition. When excited at 365 nm (within the envelope of the 355 nm band) at room temperature (10 μM concentration of **3** in $CH_3CN/H_2O$ (8:2, v/v) with HEPES as the buffer), it exhibits two weak fluorescence emission bands at $\lambda_{max}$=413 and 530 nm (Fig. 7). The band at longer wavelength is typical of an excited state intramolecular proton transfer (ESIPT) phenomenon. The general pathway of the photochromism in Schiff bases is as follows.[15] The basal enol form is excited to a (π–π*) state from where the hydroxylic proton is quickly transferred to the nitrogen of the imino atom: the resulting geometry corresponds to the fluorescent cis-keto tautomer (also a π–π* state), which may undergo relaxation toward a ground state trans-keto isomer form (photochromic tautomer). The steady state emission in such compounds is dominated by the cis-keto tautomer since the decay of the excited enol state is very fast. As compared to absorption and fluorescent studies[15] of SA (salicylideneaniline) and SN (salicylidene-1-naphthylamine) in acetonitrile, it may be stated that the tautomer responsible for the ground state absorption is the hydrogen-bonded enolic form giving a band at 355 nm; the same was found at 337 and 350 nm in SA and SN, respectively. In both SA and SN the prominent bands in the fluorescence spectra, showing large Stokes shifts appearing at 537 and 547 nm, respectively, are due to emission from the cis-keto tautomer formed after photoinduced

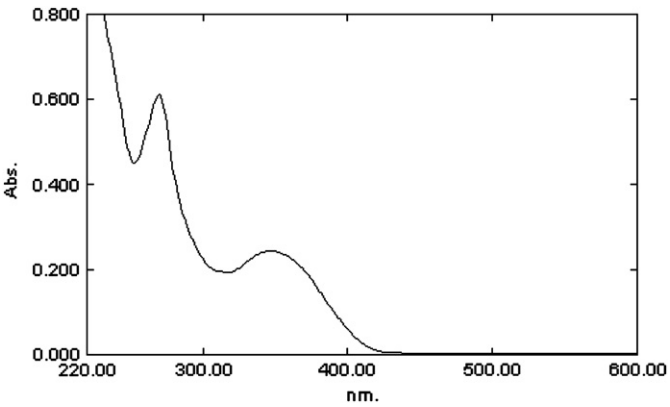


**Figure 6.** Showing absorption spectrum of **3** ($1\times10^{-5}$ M) in $CH_3CN/H_2O$ (8:2, v/v).

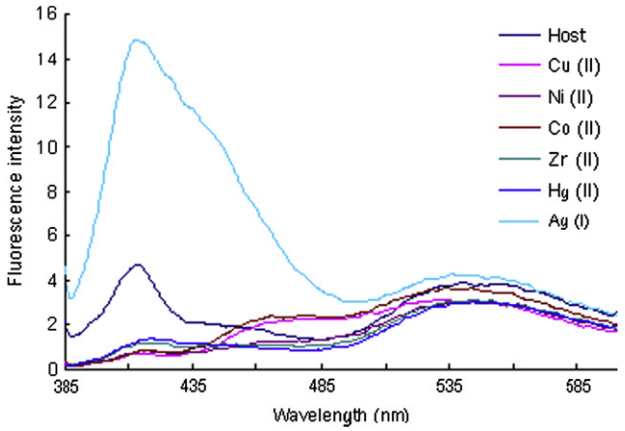


**Figure 7.** Changes in fluorescence intensity of **3** (10 μM) at $\lambda_{max}$=413 nm upon addition of 2.0 equiv of a particular metal ion salt in $CH_3CN/H_2O$ (8:2, v/v) (10 mM HEPES buffer, pH=6.2) with excitation at 365 nm.

proton transfer. The long wavelength band found in **3** at 530 nm may thus be of the same nature. In both SA and SN, apart from this main band, a weak, short wavelength emission has also been noticed, which has been associated with the emitting species preceding the appearance of the fluorescent cis-keto tautomer. The emission band observed at 413 nm in the present compound is thus assigned to intraligand $^1(\pi-\pi^*)$ fluorescence from the excited enolic state.[9e,16] The band has low intensity because of quenching due to photoinduced electron transfer (PET) mechanism, which comes into play due to the availability of the lone pairs of N of the –C=N group[9e] and O of the OH group, which cause quenching.

To evaluate the metal binding affinity of receptor **3**, the changes in fluorescence intensity of **3** upon addition of different metal salts were recorded (Fig. 7). Figures 7 and 8 clearly show that there is a marked enhancement in fluorescence intensity only upon addition of silver salt. On the other hand, no such significant changes in fluorescence spectra were observed when receptor **3a** was exposed to copper, nickel, cobalt, zinc or mercury salts under the same experimental conditions. Upon complexation of the $Ag^+$ ion, the N of the –C=N group and O of the OH group are involved in coordination with the metal ion hindering the PET phenomenon and fluorescence is restored resulting in an *off-to-on* signal. Such a phenomenon has earlier been reported in Zn(II)-sensitive fluorescent chemosensor.[9e] Both these systems work in a way similar to that found in some aminofluoresceins.[17] Thus in the present case Ag(I) increases the oxidation potential of the receptor **3**.

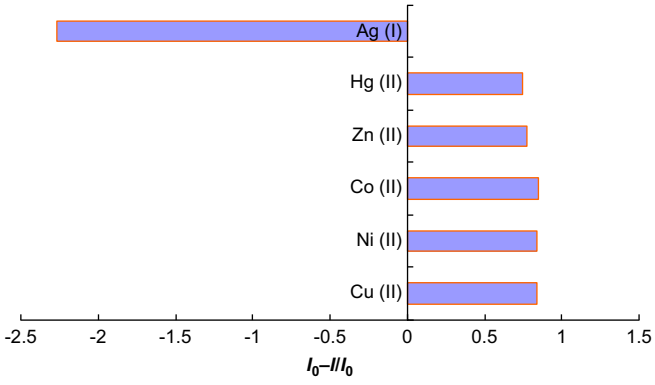


**Figure 8.** Fluorescence ratio $[(I_0-I)/I_0]$ of **3** (10 μM) at 413 nm upon addition of 2.0 equiv of a particular metal ion salt in HEPES buffered (10 mM, pH=6.2) $CH_3CN/H_2O$ (8:2, v/v), $I_0$ and $I$ are the intensities in the absence and presence of the metal ion, respectively.

To learn more about the properties of **3** as a receptor for silver, fluorescence titration was carried out. Figure 9 illustrates the emission response of chemosensor **3** with increase in concentration of $Ag^+$ ion. The fluorescence intensity of a 10 μM solution of **3** at 413 nm enhanced monotonically with a slight 'blue shift' on addition of $Ag^+$ ion into the solution, while shape of the emission band is not changed. The receptor **3** exhibited a high sensitivity toward silver, enhancing its fluorescence intensity fourfold with 2.0 equiv of silver. The association constant $K_a$ of **3** for silver was calculated on the basis of the Benesi–Hilderbrand plot[18] (Fig. 10), and it was found to be $(2.9\pm0.1)\times10^3$ $M^{-1}$. The stoichiometry of the complex formed was determined by Job's plot (Fig. 11), and it

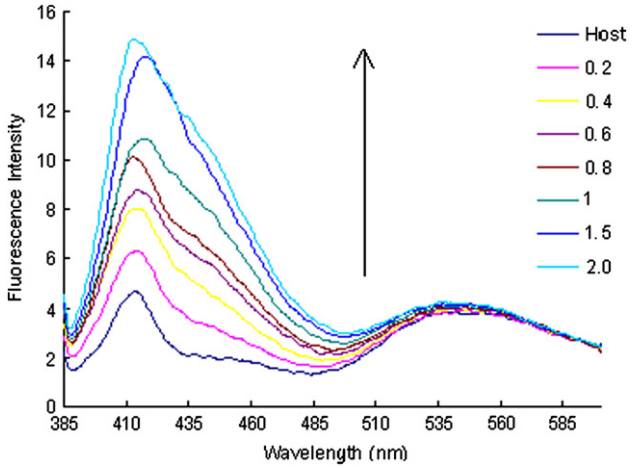


**Figure 9.** Fluorescence spectra changes of **3** (10 μM) upon addition of silver salt (0–10 μM) in HEPES buffered (10 mM, pH=6.2) $CH_3CN/H_2O$ (8:2, v/v).

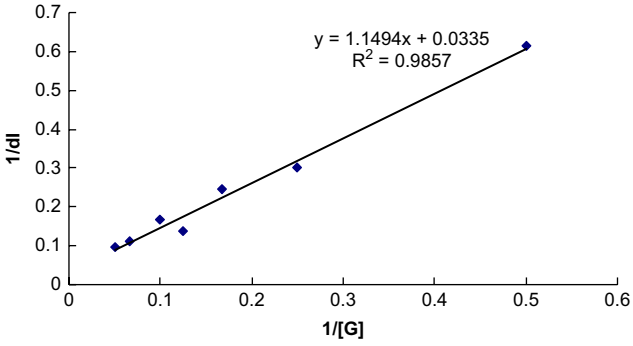


**Figure 10.** Benesi–Hilderbrand plot for the determination of stability constant of silver with the receptor **3**.

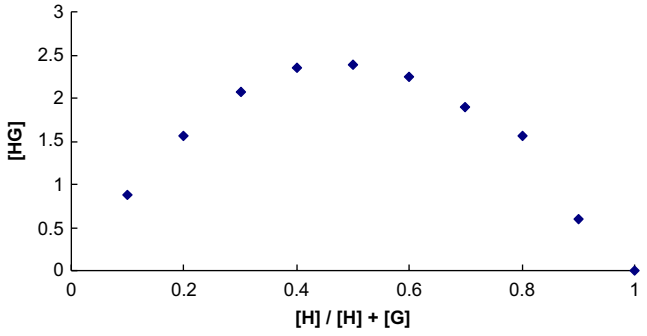


**Figure 11.** Job's plot between the receptor **3** and silver. The concentration of [HG] was calculated by the equation $[HG]=I/I_0\times[H]$.

was found to be 1:1. The smooth shape of the Job plot reflects well the rather small value of $K_s$.

## 5. NMR studies of the binding in receptors

The $^1$H NMR experiment was performed to understand the nature of receptor–$Ag^+$ interactions. A comparison of $^1$H NMR spectrum of receptor **2** and $^1$H NMR of receptor **2** mixed with 1.0 equiv of $Ag^+$ salt ($CD_3CN/CDCl_3$ (1:9, v/v) solvent system) shows lot of changes. A singlet for the $-NH_2$ protons in the free amine shifts to a higher frequency with $\Delta\delta$ 0.50 ppm. The $-CH_2S$ protons show a low frequency shift of $\Delta\delta$ 0.05 and at the same time all protons of 2-aminothiophenol and those of ethyl group show a high frequency shift in their chemical shift values (Fig. 12). The maximum shift ($\delta$ 0.28) is found for the proton attached to C6 (see Scheme 1 for atom labeling). These changes in the NMR suggest a binding of Ag(I) through amine N and S atoms. As no signal splitting was observed, it can be concluded that all the three arms of receptor are engaged in complexation.

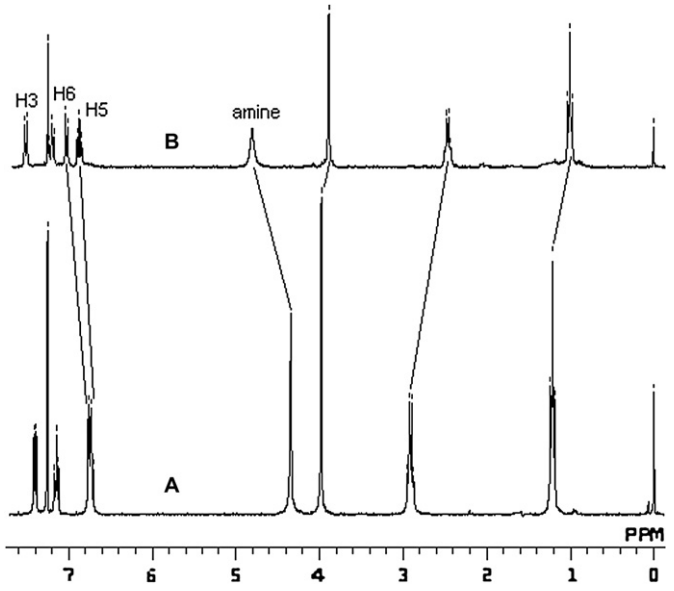


**Figure 12.** $^1$H NMR spectrum of (**A**) receptor **2** and (**B**) receptor **2**+1.0 equiv of silver salt in $CD_3CN/CDCl_3$ (1:9, v/v) solvent system.

The results of $^1$H NMR titration experiment, which was performed to decide the binding sites of receptor **3** for $Ag^+$ are shown in Figure 13. In the presence of $Ag^+$ a shift in –OH proton signal shows that this donor group plays an important role in binding to the metal ion. During the course of titration the –OH signal was gradually broadened and shifted from $\delta$ 13.13 to 12.79. Thus the signal of the –OH proton was shifted by $\Delta\delta$ 0.34. Small high frequency shifts of $\Delta\delta$ 0.02, 0.12, and 0.04 were also seen for the imine protons and the aromatic protons of the salicylaldehyde unit. However, no shift was observed for protons of the $-SCH_2$ or ethyl group suggesting the binding to be mainly through –OH group only.

## 6. Extraction and transportation studies

To evaluate a particular metal binding ability of receptors **2** and **3**, competitive solvent extraction experiments were performed. In a typical experiment, an aqueous solution containing metal salt (1.0 mM) was shaken with the host solution (2.0 mM). These experiments were carried out at neutral pH. The concentrations of metal salts left in the aqueous phase after extraction and also in blank analysis were determined by atomic absorption spectroscopy, and these values were taken as a measure to determine the percentage of metal ion extracted by the receptor. Figure 14 represents the percentage of metal ions extracted (%*E*) by the receptors **2** and **3**, which clearly shows that both the receptors have higher complexation ability for $Ag^+$ than for any other metal ion, with receptor **3** being better than receptor **2.** As receptor **3** has an imine linkage, which tends to hydrolyze, so this receptor is not a good candidate for studies to be carried out at low pH value. Thus, we selected only the receptor **2** for pH dependent metal extraction and transport studies.

Extraction experiments help to determine the efficiencies of a receptor to complex metal ions at the interface of aqueous source phase and organic layer. However, a higher extraction ability of any receptor alone does not warrant its use for applications in

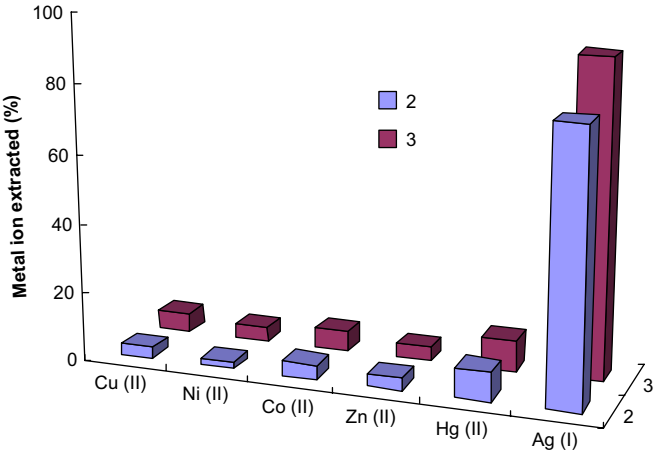


**Figure 14.** Competitive solvent extraction (%*E*) of various metal ions with the receptors **2** and **3**.

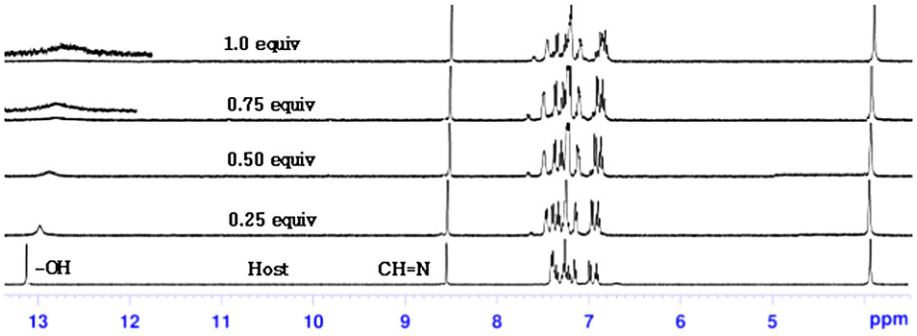


**Figure 13.** Partial $^1$H NMR spectra of receptor **3** on addition of silver salt in $CD_3CN/CDCl_3$ (1:9, v/v) on a 400 MHz Bruker instrument.

separation chemistry. If a receptor forms a very strong complex with a particular metal ion and yet the decomplexation of metal ions from the receptor is not possible, then the receptor will be wasted after a single use. Thus, metal decomplexation from a receptor is also important. For the determination of decomplexation of metal from the receptor **2**, a decomplexation experiment was performed by extracting the organic layer from the extraction experiment with hydrochloric acid (at pH 1). The data are expressed as the percentage of $Ag^+$ ion decomplexed from the receptor **2** (Fig. 15). The concentration of metal salt released to the acidic aqueous phase was determined by atomic absorption spectroscopy.

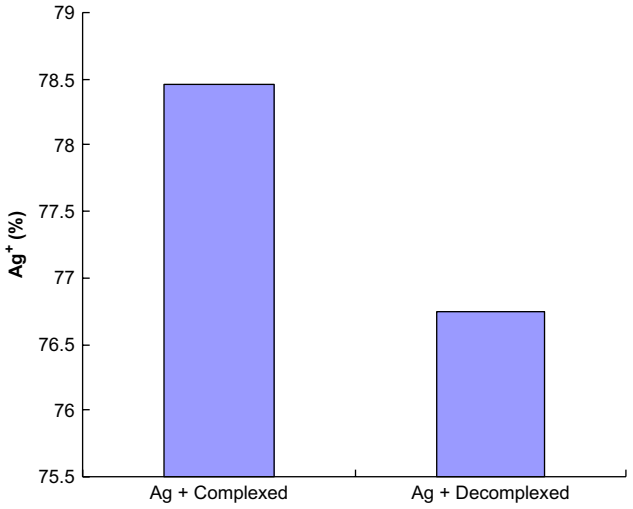


**Figure 15.** Comparison of $Ag^+$ extraction (%*E*) and decomplexation (%*D*) efficiencies of the receptor **2**.

Figure 15 shows that the decomplexation ability of the receptor for $Ag^+$ is almost as good as its complexation. The majority of the extracted metal ions was released when the organic layer containing the metal–receptor complex was shaken with hydrochloric acid (at pH 1). Due to the high acidity, the protons compete for the amine nitrogens and metal ions are released at a high rate. Receptor **2** was also tested for its reuse in extracting $Ag^+$ from the buffered aqueous phase. Before reuse, the receptor was neutralized with a base. Figure 16 shows that **2** can be reused effectively for the extraction of $Ag^+$ and its extraction efficiency only decreased a little after being used five times.

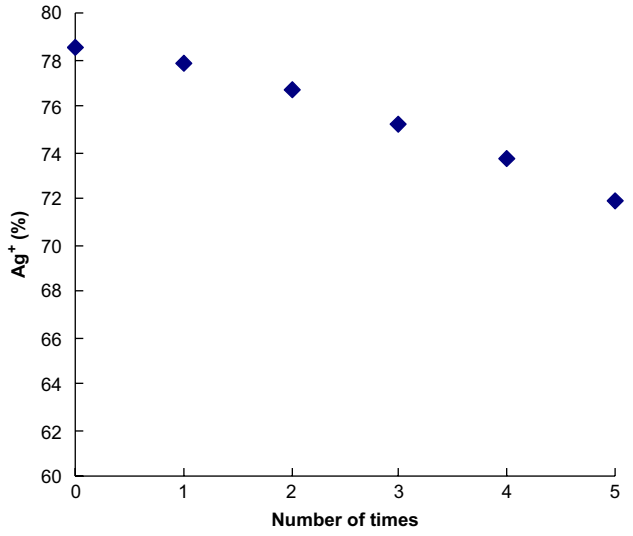


**Figure 16.** Reuse of receptor **2** for the extraction of $Ag^+$.

Transport experiments involve complexation at the interface of the source aqueous phase and the organic layer, while decomplexation occurs at the interface of the organic layer and the receiving aqueous phase. Hence a transport experiment is a continuous process of metal extraction and metal decomplexation. A slow decrease in the concentration of metal ions in the source aqueous phase signifies the inability of a receptor to extract ions from the aqueous phase. On the other hand, a slow increase in the concentration of ions in the receiving aqueous phase reflects a difficulty in the release of the metal ions. We examined the transport ability of receptor **2** by taking a carrier in the chloroform layer and metal ions in the aqueous buffer phase (source phase). In these transport experiments, the concentrations of the carrier in the membrane and of the metal ions in the buffer source phase (pH=4.6) were 1 and 5 mM, respectively. Hydrochloric acid (pH 1) was used for the receiving phase. The concentration of $Ag^+$ was monitored in both aqueous compartments (i.e., both in the source phase and in the receiving phase) with atomic absorption spectroscopy. To find the efficiency of the receptor properly, it is necessary to find out the time dependence of the transportation in both the phases. Therefore, the percentage of metal ion transported was monitored as a function of time. Each reading was taken after a time interval of 2 h for 12 h and then after 24 h. This makes it possible to estimate the rate of transportation of $Ag^+$ ion and also the total time required (Fig. 17). The data show that the transport rate is fast for the first 4 h and then after next 4 h (i.e., after total 8 h) most of the $Ag^+$ has been transported. The actual transport rate has been calculated to be $1140\times10^{-7}$ M/l/day.

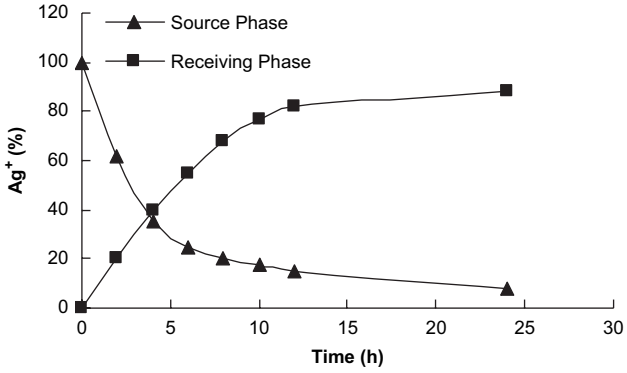


**Figure 17.** Transport rate of $Ag^+$ as a function of time.

Studies on aza-thioethers have revealed that presence of S and N atoms in the macrocycle facilitate the coordination Ag(I) and thus help in extraction of metal ion.[19] In functionalized thioethers the functional group attached to the pendent helps in the extraction by coordination to metal ion as well stabilizations of anion by H-bonding with the group on the pendent. It appears that in the present study receptor **2** mimics the aza-thioethers as far as coordination of S and N atoms with Ag(I) is concerned. However the receptor **3** adopts different coordination modes with Ag(I) and major coordination sites appear to be mainly through –OH groups.

## 7. Conclusions

Silver(I) ion selectivity and specificity of the Schiff base **3** has been optically transduced by the receptor-cum-reporter imine unit. This has been achieved by avoiding the appendage of any special fluorophore unit to the molecule, just by using the weak

fluorescence property of the Schiff base itself. The fluorogenic chemosensor was selective and sensitive for Ag(I), capable of detecting the metal ion in a concentration of $1\times10^{-5}$ M with the help of spectrophotometer, in the presence of other interfering metal ions. The tripodal amine **2** has been successfully used to extract and transport Ag(I) and the receptor has been shown to be useful for repeated extraction and transportation experiments.

## 8. Experimental

### 8.1. General

All solvents were dried by standard methods. Unless otherwise specified, chemicals were purchased from Sigma Aldrich and used without further purification. TLC was performed on glass sheets pre-coated with silica gel (Kieselgel 60 PF254, Merck). The elemental analyses were performed on a Flash EA 1112 elemental analyzer. The $^1$H NMR spectra were either recorded on a 300 MHz JEOL or 400 MHz Bruker spectrometer, in $CDCl_3$ or $CD_3CN$–$CDCl_3$ (2:8) mixture. $^{13}$C NMR were run on a 75 MHz JEOL machine. The chemical shifts are reported as $\delta$ values (ppm) relative to TMS. IR spectra were recorded on a PYE Unicam IR spectrometer for the compounds in the solid state as KBr discs or as neat samples. TMS was used as an internal reference. A Perkin–Elmer A Analyst100 atomic absorption spectrometer was used for the measurement of concentrations of the analytes in extraction and transportation experiments. The absorption spectra were recorded on a Shimadzu UV-1700 UV–vis spectrophotometer. The fluorescence measurements were performed on a Perkin Elmer LS55 Luminescence Spectrometer.

### 8.2. Compound 2

Tripodal amine **2** was prepared by taking $K_2CO_3$ (1 g, mmol) in dry acetonitrile along with 2-aminothiophenol (375 mg, 3.0 mmol). The reaction mixture was refluxed for 20 min and then tribromide **1** (440 mg, 1 mmol) was carefully added to it. The reaction mixture was refluxed for next 8 h and the progress of the reaction was monitored by TLC. Upon completion of reaction, $K_2CO_3$ was filtered off and whole of the acetonitrile was evaporated. The crude product was recrystallized from chloroform–methanol solvent mixture to get a pure white material. Yield 47%; mp 87 °C; IR (KBr, $cm^{-1}$) 1306 (s), 1604 (s), 2884 (s), 3388 (w), 3469 (w); $^1$H NMR (300 MHz, $CDCl_3$, ppm) $\delta$: 1.21 (9H, t, $J$=7.5 Hz, $-CH_3$), 2.91 (6H, q, $J$=7.5 Hz, $-CH_2$), 3.98 (6H, s, $-CH_2$), 4.35 (6H, s, $-NH_2$), 6.71–6.77 (6H, m, Ar), 7.15 (3H, t, Ar, $J$=8.0), 7.40 (3H, d, Ar, $J$=7.5); $^{13}$C NMR (75 MHz, $CDCl_3$) $\delta$: 16.1 ($-CH_3$), 22.8 ($-CH_2$), 34.5 ($-CH_2$), 115.0 (Ar), 118.5 (Ar), 118.7 (Ar), 129.8 (Ar), 131.2 (Ar), 135.6 (Ar), 142.9 (Ar), 148.5 (Ar). CHN Anal. Calcd % for $C_{33}H_{39}N_3S_3$: C, 69.07; H, 6.85; N, 7.32. Found C, 69.09; H, 7.12; N, 7.23.

### 8.3. Compound 3

This compound was prepared by stirring tripodal amine **2** (573 mg, 1.0 mmol) along with salicylaldehyde (390 mg, 3.2 mmol) in the presence of traces of zinc perchlorate taken in acetonitrile–chloroform (9:1) solvent mixture. The color of the solution changed immediately to yellow and precipitate separated out in quantitative yield upon addition of methanol. These precipitates were filtered and dried. Yield 58%; mp=197 °C; IR (KBr, $cm^{-1}$) 1613 (s), 3419 (br m); $^1$H NMR (300 MHz, $CDCl_3$) $\delta$: 1.17 (t, 9H, $-CH_3$, $J$=7.5 Hz), 2.63 (q, 6H, $-CH_2$, $J$=7.5 Hz), 3.92 (s, 6H, $-CH_2$), 6.89–6.99 (m, 6H, Ar), 7.13–7.40 (m, 18H, Ar), 8.54 (s, 3H, –CH=N), 13.14 (s, 3H, –OH,); $^{13}$C NMR (75 MHz, $CDCl_3$): $\delta$ 16.2 ($-CH_3$), 22.9 ($-CH_2$), 32.1 ($-CH_2$), 117.3 (Ar), 118.1 (Ar), 118.9 (Ar), 119.3 (Ar), 127.3 (Ar), 129.0 (Ar), 130.2 (Ar), 131.2 (Ar), 132.4 (Ar), 133.0 (Ar), 137.0 (Ar), 143.7 (Ar), 154.4 (Ar), 161.2 (Ar), 162.4 (CH=N), 172.6 (Ar–OH). Anal. Calcd % for $C_{54}H_{51}N_3O_3S_3$: C, 73.19; H, 5.80; N, 4.74. Found: C, 72.94; H, 6.01; N, 4.84.

### 8.4. Competitive solvent extraction (%*E*)

The percentage extraction (%$E$) of the metal salt extracted from the aqueous solution containing metal salts ($1.0\times10^{-3}$ M, 2.0 ml) to the chloroform layer containing a receptor ($2.0\times10^{-3}$ M, 2.0 ml) was determined at 25 °C. The aqueous and organic mixtures were shaken vigorously for a few minutes and the mixtures were left to stand until phase separation was completed. Similarly, the blank analysis was performed by taking metal salts ($1.0\times10^{-3}$ M, 2.0 ml) dissolved in the aqueous solution and 2.0 ml of neat chloroform. The concentration of the metal salts in the aqueous solution was determined after extraction and also in blank analysis by an atomic absorption spectrometer. The percentage extraction (%$E$) of metal salts was determined by the formula $\%E=(C_1-C_2)\times100/C_1$, where $C_1$ is the concentration of metal salts in the aqueous buffer solution in blank analysis, and $C_2$ is the concentration of metal salts remaining in aqueous buffer solution after extraction. An average value of three independent determinations is reported.

### 8.5. Decomplexation of metal ion (%*D*)

The percentage decomplexation (%$D$) of the metal salt from the chloroform layer (containing complex 2.0 ml) to hydrochloric acid was determined at 25 °C. The chloroform layer of a competitive solvent extraction experiment separated from the aqueous layer was selected. This organic layer was shaken with 2.0 ml of hydrochloric acid (pH=1.0), and the solution was kept undisturbed until complete separation had occurred. The concentration of metal salt in hydrochloric acid was determined on an atomic absorption spectrometer. The percentage decomplexation (%$D$) of metal salt was determined by the formula $\%D=(C_3/C_1)\times100$, where $C_1$ is the concentration of metal salts in the aqueous buffer solution in blank analysis of competitive solvent extraction experiment, and $C_2$ is the concentration of metal salts released to 0.1 M HCl. An average value of three independent determinations is reported.

### 8.6. pH Dependent transport experiment

Transport experiments were carried out by stirring the organic phase of bulk liquid membrane cell at a constantly slow speed so that the interfaces between the organic membrane and two aqueous phases remained flat and well defined. The two aqueous phases were separated by the organic phase. An aqueous source phase (4.0 ml) containing $Ag^+$ ($5\times10^{-3}$ M) in acetate buffer (pH=4.6) and a receiving phase (8.0 ml) containing HCl (pH=1.0) were separated by the organic layer of chloroform (25 ml) containing a carrier ($1\times10^{-3}$ M). The concentration of the carrier in the transport cell containing compound **2** was $2\times10^{-3}$ M. The metal ion concentrations in both aqueous phases were monitored with an atomic absorption spectrophotometer. An average value of three independent determinations is reported.

### 8.7. Stability constant determination

The stability constant of receptor **3** with silver was determined by preparing solutions containing 10 μM of receptor **3** and varying amounts (0–20 μM) of silver salt in $CH_3CN/H_2O$ (8:2, v/v) (10 mM HEPES buffer, pH=6.2). The emission was measured at 413 nm.

### 8.8. Stoichiometry determination

Mixtures of receptor–silver salt were prepared as 1:9, 2:8, 3:7, 4:6, 5:5, 6:4, 7:3, 8:2, 9:1. These solutions were kept at 25+1 °C

before recording their spectra. The plot of [HG] versus [H]/[H]+[G] was used to determine the stoichiometry of the complex formed. The concentration of [HG] was calculated by the equation $[HG]=\Delta I/I_0\times[H]$.

### 8.9. X-ray crystallography and structure determination

The data for both the crystals were collected on a Siemens P4 single crystal X-ray diffractometer, using Mo Kα radiation (0.71609 Å). Table 1 gives the details of data collection and refinement for both **2** and **3**. Both structures were solved by direct methods and subsequently by difference Fourier Syntheses and refined by full-matrix least-squares on $F^2$ with WINGX.[20] Lorentz and polarization corrections were applied but no absorption correction was applied. All non-hydrogen atoms were refined anisotropically. Hydrogens were fixed geometrically and were not refined. They were made to ride on their respective atoms with thermal parameters 1.5 times for a methyl carbon and 1.2 times for methylene and aromatic carbons. The H-bonding calculations, torsion and dihedral angles and plane were calculated by using PARST.[21]

## Acknowledgements

G.H. and V.K.B. are thankful to the CSIR, India for research grant No. 01(2104)/07/EMR-II and research fellowship, respectively.

## Supplementary data

Supplementary data associated with this article can be found in the online version, at doi:10.1016/j.tet.2008.03.013.

## References and notes

1. (a) Basabe-Desmonts, L.; Reinhoudt, D. N.; Crego-Calama, M. *Chem. Soc. Rev.* **2007**, *36*, 993–1017; (b) de Silva, A. P.; Gunaratne, H. Q. N.; Gunnlaugsson, T.; Huxley, A. J. M.; McCoy, C. P.; Rademacher, J. T.; Rice, T. E. *Chem. Rev.* **1997**, *97*, 1515–1566; (c) *Fluorescent Chemosensors for Ion and Molecule Recognition*; Desvergne, J. P., Czarnik, A. W., Eds.; Kluwer Academic: Dordrecht, The Netherlands, 1997; (d) Prodi, L.; Bolletta, F.; Montalti, M.; Accheroni, N. *Coord. Chem. Rev.* **2000**, *205*, 59–83.
2. (a) Martinez, R.; Espinosa, A.; Tarraga, A.; Molina, P. *Org. Lett.* **2005**, *7*, 5869–5872 and Refs. 4 and 5 therein; (b) Guo, X.; Qian, X.; Jia, L. *J. Am. Chem. Soc.* **2004**, *126*, 2272–2273; (c) Wang, L.; Zhu, X.-J.; Wong, W.-Y.; Guo, J.-P.; Wong, W.-K.; Li, Z.-Y. *J. Chem. Soc., Dalton Trans.* **2005**, 3235–3240; (d) Player, T. N.; Shinoda, S.; Tsukube, H. *Org. Biomol. Chem.* **2005**, *3*, 1615–1616; (e) Gunnlaugsson, T.; Kruger, P. E.; Lee, T. C.; Parkesh, R.; Pfeffer, F. M.; Hussey, M. G. *Tetrahedron Lett.* **2003**, *44*, 6575–6578; (f) Gunnlaugsson, T.; Davis, A. P.; Glynn, M. *Chem. Commun.* **2001**, 2556–2557; (g) Descalzo, A.; Martinez-Mañez, R.; Radeglia, R.; Rurack, K.; Soto, J. *J. Am. Chem. Soc.* **2003**, *125*, 3418–3419.
3. (a) McClure, D. S. *J. Chem. Phys.* **1952**, *20*, 682–686; (b) Varnes, A. V.; Dodson, R. B.; Whery, E. L. *J. Am. Chem. Soc.* **1972**, *94*, 946–950; (c) Kemlo, J. A.; Shepherd, T. M. *Chem. Phys. Lett.* **1977**, *47*, 158–162; (d) Rurack, K.; Resch, V.; Senoner, M.; Dachne, S. *J. Fluoresc.* **1993**, *3*, 141–143; (e) Prodi, L.; Bolletta, F.; Montalti, M.; Zaccheroni, N. *Coord. Chem. Rev.* **2000**, *205*, 59–83; (f) Valeur, B.; Leary, I. *Chem. Rev.* **2000**, *205*, 3–40.
4. Kubo, K. PET Sensors. In *Advanced Concepts in Fluorescence Sensing. Part A: Small Molecule Sensing*; Geddes, C. D., Lakowicz, J. R., Eds.; Topics in Fluorescence Spectroscopy; Springer: New York, NY, 2005; Vol. 9, pp 219–243.
5. Chattopadhyay, N.; Mallick, A.; Sengupta, S. *J. Photochem. Photobiol., A* **2005**, *177*, 55–60.
6. Anslyn, E. V. *J. Org. Chem.* **2007**, *72*, 687–699.
7. de Silva, A. P.; McCaughan, B.; McKinney, B. O. F.; Querol, M. *Dalton Trans.* **2003**, *10*, 1902–1913.
8. (a) Vance, D. H.; Czarnik, A. W. *J. Am. Chem. Soc.* **1994**, *116*, 9397–9398; (b) de Silva, A. P.; Gunaratne, H. Q. N.; Gunnalugsson, T.; Nieuwenhuizen, M. *Chem. Commun.* **1996**, 1967–1968.
9. (a) Lo, W.-K.; Wong, W.-K.; Wong, W.-Y.; Guo, J.; Yeung, K.-T.; Cheng, Y.-K.; Yang, X.; Jones, R. A. *Inorg. Chem.* **2006**, *45*, 9315–9325; (b) Okabe, C.; Nakabayashi, T.; Inokuchi, Y.; Nishi, N.; Sekiya, H. *J. Chem. Phys.* **2004**, *121*, 9436–9442; (c) Otsubo, N.; Okabe, C.; Mori, H.; Sakota, K.; Amimoto, K.; Kawato, T.; Sekiya, H. *J. Photochem. Photobiol., A* **2002**, *154*, 33–39; (d) Fujiwara, T.; Harada, J.; Ogawa, K. *J. Phys. Chem. B* **2004**, *108*, 4035–4038; (e) Gao, L.; Wang, Y.; Wang, J.; Huang, L.; Shi, L.; Fan, X.; Zou, Z.; Yu, T.; Zhu, M.; Li, Z. *Inorg. Chem.* **2006**, *45*, 6844–6850; (f) Ohshima, A.; Momotake, A.; Arai, T. *J. Photochem. Photobiol., A* **2004**, *162*, 473–479; (g) Ziólek, M.; Kubicki, J.; Maciejewski, A.; Naskrecki, R.; Grabowska, A. *Phys. Chem. Chem. Phys.* **2004**, *6*, 4682–4689; (h) Yu, T.; Zhang, K.; Zhao, Y.; Yang, C.; Zhang, H.; Fan, D.; Dong, W. *Inorg. Chem. Commun.* **2007**, *10*, 401–403 and Refs. 6–18 therein; (i) Ghosh, R.; Rahaman, S. H.; Rosair, G. M.; Ghosh, B. K. *Inorg. Chem. Commun.* **2007**, *10*, 61–65; (j) Yu, T.; Zhang, K.; Zhao, Y.; Yang, C.; Zhang, H.; Qian, L.; Fan, D.; Dong, W.; Chen, L.; Qiu, Y. *Inorg. Chim. Acta.* **2008**, *361*, 233–240; (k) Abe, A. M. M.; Helaja, J.; Koskinen, A. M. P. *Org. Lett.* **2006**, *8*, 4537–4540.
10. (a) Bhardwaj, V. K.; Singh, N.; Hundal, M. S.; Hundal, G. *Tetrahedron* **2006**, *62*, 7878–7886; (b) Singh, N.; Hundal, M. S.; Hundal, G.; Martinez-Ripoll, M. *Tetrahedron* **2005**, *61*, 7796–7806; (c) Singh, N.; Hundal, G. *J. Inclusion Phenom. Macrocycl. Chem.* **2005**, *52*, 253–259; (d) Singh, N.; Kumar, M.; Hundal, G. *Tetrahedron* **2004**, *60*, 5393–5405; (e) Singh, N.; Kumar, M.; Hundal, G. *Inorg. Chim. Acta* **2004**, *357*, 4286–4290.
11. (a) Rurack, K.; Kollmannsberger, M.; Resch-Genger, U.; Daub, J. *J. Am. Chem. Soc.* **2000**, *122*, 968–969; (b) Tong, H.; Wang, L.; Jing, X.; Wang, F. *Macromolecules* **2002**, *35*, 7169–7171; (c) Chae, M.-Y.; Czarnik, A. W. *J. Am. Chem. Soc.* **1992**, *114*, 9704–9705.
12. Cabell, L. A.; Best, M. D.; Lavigne, J. J.; Schneider, S. E.; Perreault, D. M.; Monahan, M.-K.; Anslyn, E. V. *J. Chem. Soc., Perkin Trans. 2* **2001**, 315–323.
13. Sun, W. Y.; Fan, J.; Okumura, T.-A.; Xie, J.; Yu, K. B.; Ueyama, N. *Chem.—Eur. J.* **2001**, *7*, 2557–2562.
14. (a) Lo, W.-K.; Wong, W.-K.; Guo, J.-P.; Wong, W.-Y.; Li, K.-F.; Cheah, K.-W. *Inorg. Chim. Acta* **2004**, *357*, 4510–4521; (b) Gilli, P.; Bertolasi, V.; Ferretti, V.; Gilli, G. *J. Am. Chem. Soc.* **2000**, *122*, 10405–10417; (c) Bertolasi, V.; Gilli, P.; Ferretti, V.; Gilli, G. *J. Am. Chem. Soc.* **1991**, *113*, 4917–4925; (d) Filarowski, A.; Koll, A.; Glowiak, T. *J. Chem. Soc., Perkin Trans. 2* **2002**, 835–847.
15. Rodriguez-Cordoba, W.; Zugazagoitia; Collado-Fregoso, E.; Peon, J. *J. Phys. Chem. A* **2007**, *111*, 6241–6247.
16. (a) Dutta, B.; Bag, P.; Florke, U.; Nag, K. *Inorg. Chem.* **2005**, *44*, 147–157; (b) Kang, Y.; Zhang, J.; Li, Z.-J.; Qin, Y.-Y.; Yao, Y.-G. *Inorg. Chem. Commun.* **2005**, *8*, 722–724.
17. (a) Hirano, T.; Kikuchi, T.; Urano, Y.; Higuchi, T.; Nagano, T. *Angew. Chem., Int. Ed.* **2000**, *39*, 1052–1054; (b) El Haskouri, J.; Ortiz de Zárate, D.; Guillem, C.; LaTorre, J.; Caldés, M.; Beltrán, A.; Beltrán, D.; Descalzo, A. B.; Rodríguez-López, G.; Martínez-Máñez, R.; Marcos, M. D.; Amorós, P. *Chem. Commun.* **2002**, 330–331.
18. (a) Benesi, H. A.; Hilderbrand, J. H. *J. Am. Chem. Soc.* **1949**, *71*, 2703–2704; (b) Kao, T.-L.; Wang, C.-C.; Pan, Y.-T.; Shiao, Y.-J.; Yen, J.-Y.; Shu, C.-M.; Lee, G.-H.; Peng, S.-M.; Chung, W.-S. *J. Org. Chem.* **2005**, *70*, 2912–2920.
19. Glenny, M. W.; Blake, A. J.; Wilson, C.; Schröder, M. *J. Chem. Soc., Dalton Trans.* **2003**, 1941.
20. Farrugia, L. J. *J. Appl. Crystallogr.* **1999**, *32*, 837–838.
21. (a) Nardelli, M. *Comput. Chem.* **1983**, *7*, 95–97; (b) Nardelli, M. *J. Appl. Crystallogr.* **1995**, *28*, 659.